Current Applied Science and Technology e-ISSN: 2586-9396

Curr. Appl. Sci. Technol. ….., Vol... (No...), e0269361

Research article

The Effect of the Concentration of Pineapple Peel-based ZnO/Zein Nanocomposite on the Antibacterial Activity of *Staphylococcus aureus* and *Streptococcus mutans*

Woro Setyarsih[1], Mohamad Wafiq Nafii Alfan[1], Fitriana[1], Tukiran[2], Erlix Rakhmad Purnama[3], Prima Nerito[4], R Sabda Alam[4] and Lydia Rohmawati[1]*

[1]Physics Department, Universitas Negeri Surabaya, Ketintang, Surabaya 60231, Indonesia
[2]Chemistry Department, Universitas Negeri Surabaya, Ketintang, Surabaya 60231, Indonesia
[3]Biology Department, Universitas Negeri Surabaya, Ketintang, Surabaya 60231, Indonesia
[4]Dentistry Department, Universitas Muhammadiyah Surabaya, Sutorejo, Surabaya 60113, Indonesia

Received: 30 September 2025, Revised: 14 Febuary 2026, Accepted: 12 April 2026, Published: 20 July 2026

Abstract

ZnO nanoparticles are known to have good antibacterial properties. However, because the particles are prone to agglomeration, their effectiveness can decrease, particularly when they are used as an active ingredient in mouthwash. To address this issue, ZnO nanoparticles were synthesized via green synthesis using pineapple peel (*Ananas comosus* L.) extract and subsequently combined with Zein polymer through a mixing method to form a nanocomposite, thereby minimizing agglomeration. The concentration of ZnO/Zein nanocomposite affects its ability to inhibit bacterial growth, especially on *S. aureus* and *S. mutans*. The results obtained showed that the ZnO/Zein nanocomposite composition of 1:2 at a concentration of 2.5% was the most effective in inhibiting *S. aureus* bacteria with an inhibition zone of 9.4±0.26 mm. For *S. mutans*, nanocomposites with a composition of 1:2 and 1:3 at a concentration range of 0.5-2.5% exhibited a relatively stable inhibition ability, ranging from 5.53 to 7.20 mm, which was better than that of pure ZnO. Although the antibacterial activity of the nanocomposite was lower than that of mouthwash containing 0.2% chlorhexidine, it still showed potential as a bacterial inhibitor. It is hoped that this ZnO/Zein nanocomposite can be used as an additive in antibacterial mouthwash formulations.

Keywords: ZnO/Zein nanocomposite; antibacterial; concentration; *S. aureus*; *S. mutans*, mouthwash

*Corresponding author: E-mail: lydiarohmawati@unesa.ac.id
https://doi.org/10.55003/cast.2026.269361

1. Introduction

Poor oral hygiene habits and awareness can trigger the growth of pathogenic bacteria, including *S. mutans*, which cause cavities, and *S. aureus*, which causes swollen gums (Kim et al., 2024). These bacteria can also be found on unclean oral hygiene tools, such as contaminated toothbrushes. When a toothbrush is used, bacteria can enter the oral cavity, grow, and colonize, leading to bad breath (Murukesan et al., 2023). Therefore, using mouthwash is one method to reduce bacterial growth and development (Afra & Modaresi, 2017). One antibacterial ingredient often found in mouthwash is chlorhexidine, which can kill and inhibit various bacteria found in dental plaque (Pillai et al., 2023). However, excessive use of this mouthwash can cause side effects such as tooth staining, allergic reactions, and microbial imbalance. In the long term, it can also cause tartar buildup, taste disturbances, burning sensations, and irritation of the oral mucosa (Deus & Ouanounou, 2022; Brookes et al., 2023). Due to the side effects of chlorhexidine in this mouthwash, its use is limited to around 0.2%. Therefore, alternative ingredients with antibacterial properties with minimal side effects are needed.

Several researchers reported that mouthwash containing ZnO nanoparticles exhibited high antibacterial activity against *S. mutans* and had the potential to serve as an alternative to chlorhexidine-based mouthwash for plaque control (Kachoei et al., 2018; Eslami et al., 2021). However, its toxicity and safety at various concentrations still need to be further evaluated. ZnO nanoparticles have the potential to act as antibacterial agents and are used in oral care products such as mouthwash (Osorio et al., 2011; Carrouel et al., 2020). Mouthwashes containing zinc salts (zinc gluconate, zinc chloride) or ZnO nanoparticles have shown high in vitro antibacterial activity against *S. mutans* (Almoudi et al., 2018). They may even prevent plaque accumulation, making this material an alternative to 0.2% chlorhexidine and 0.05% sodium fluoride under certain conditions (Kachoei et al., 2018). ZnO nanoparticles synthesized from plant extracts have demonstrated significant antibacterial effectiveness against various pathogens (Brunello et al., 2022). These nanoparticles can be synthesized using a green method, such as the employment of pineapple peel extract as a bioreductant (Rohmawati et al., 2024a; Setyarsih et al., 2025). The bioactive compounds in pineapple peel, including saponins, flavonoids, tannins, anthocyanins, vitamin C, carotenoids, and the enzyme bromelain, act as both reducing and capping agents, helping to prevent particle agglomeration and facilitating the formation of stable nanoparticles.

The antibacterial properties of ZnO arise from several mechanisms, including the release of Zn^{2+} ions, the formation of reactive oxygen species (ROS), and the disruption and penetration of bacterial membranes. These processes can lead to DNA damage, mitochondrial dysfunction, protein oxidation, and leakage of essential intracellular components (Kim et al., 2022; Puspasari et al., 2022; Zare et al., 2022). The amount of Zn^{2+} released into the medium is influenced by particle size and suspension concentration (Naqvi et al., 2019). Smaller ZnO particles in a moderately concentrated suspension tend to release more Zn^{2+} ions, thereby enhancing their ability to inhibit microbial growth, because small particles have a relatively higher surface area-to-volume ratio, resulting in more surface atoms and increased solubility (Naqvi et al., 2019). However, ZnO nanoparticles are prone to agglomeration, which can diminish their dispersibility and overall antimicrobial performance. To address this issue, biopolymers such as Zein can be incorporated, as they help prevent nanoparticle aggregation and may further enhance the antimicrobial effect against microorganisms (Naguib et al., 2021).

Zein is a natural, biodegradable, and biocompatible protein derived from corn that functions as a carrier or matrix for antimicrobial nanoparticles. This biopolymer can form films or nanoparticles that gradually release active substances, thereby enhancing the effectiveness and stability of antimicrobial agents, such as ZnO, in mouthwash formulations (Kasper et al., 2016). Zein modified to coat thymol (a natural phenolic compound) demonstrated antimicrobial efficacy by disrupting bacterial biofilms and increasing antibiotic penetration (de Almeida Campos et al., 2023). Bortoletto-Santos et al. (2018) reported that ZnO coated with Zein exhibited good antimicrobial activity. This material can be developed for packaging applications because it shows high antibacterial activity and long-term performance against both gram-negative and gram-positive bacteria (Cao et al., 2017). These studies indicate that the ZnO/Zein combination can improve mechanical, thermal, and barrier properties. However, research on ZnO and Zein combinations remains relatively limited, offering an opportunity to further investigate their potential as antibacterial agent in mouthwash, particularly for inhibiting the growth of *S. aureus* and *S. mutans*. The findings of this research are expected to support the development of ZnO/Zein nanocomposite formulations for potential applications in mouthwash.

2. Materials and Methods

The materials that need to be prepared in the research include distilled water, pineapple peel (*Ananas comosus L.*), zinc acetate dihydrate (Zn $(CH_3COOH)_2 \cdot 2H_2O$, Merck), NaOH (Sigma Aldrich), Zein polymer (Sigma Aldrich), 96% ethanol (Merck), Polyvinyl Alcohol (PVA, Merck). In carrying out the research, the tools needed are a mortar and pestle, a glass and an iron spatula, a 200-mesh sieve, a beaker, a stirrer, a drying oven, a digital scale, a measuring cup, a Whatman filter paper, aluminum foil, a petri dish, a centrifuge, a sonicator, and a 250 mL beaker.

2.1 Fabrication of ZnO/Zein nanocomposites

Before preparing the ZnO/Zein nanocomposite, ZnO nanoparticles were first synthesized using the green synthesis method, as described in previous research (Rohmawati et al., 2024a). The stages of this process are illustrated in Figure 1. The pineapple skin was first peeled; the pericarp was separated and then washed using distilled water to remove dust and dirt. A total of 10 g of pineapple skin was put into 100 mL of distilled water.

The mixture was stirred at 80°C for 1 h using a stirrer. After that, the solution was cooled to room temperature and filtered to separate solid lumps. From the resulting yellow solution, 50 mL was taken, and then 10 mL of distilled water and 4 g of zinc acetate dihydrate were added. The mixture was sonicated at 40°C for 1 h until it reached an alkaline pH (approximately 10-13). Then, 100 mL of NaOH solution was added, and the mixture was centrifuged. The precipitate obtained was then dried in an oven at 120°C for 12 h, yielding ZnO powder. It should be noted that the use of pineapple peel extract in the green synthesis of ZnO nanoparticles as a bioreduction and capping agent (Rohmawati et al., 2025), to help stabilize Zn^{2+} ions, accelerate ZnO nucleation and prevent agglomeration so that uniform nano sizes are formed (Klinbumrung et al., 2022; Rohmawati et al., 2024a). In this case, zinc ions from zinc acetate are reduced by the hydroxyl groups of phenolic compounds, flavonoids, and polysaccharides of pineapple peel extract, which form zinc metal particles, which are then oxidized by NaOH into ZnO nanoparticles and stabilized by organic molecules (Klinbumrung et al., 2022). The chemical reactions during the green synthesis process of ZnO nanoparticles are as follows:

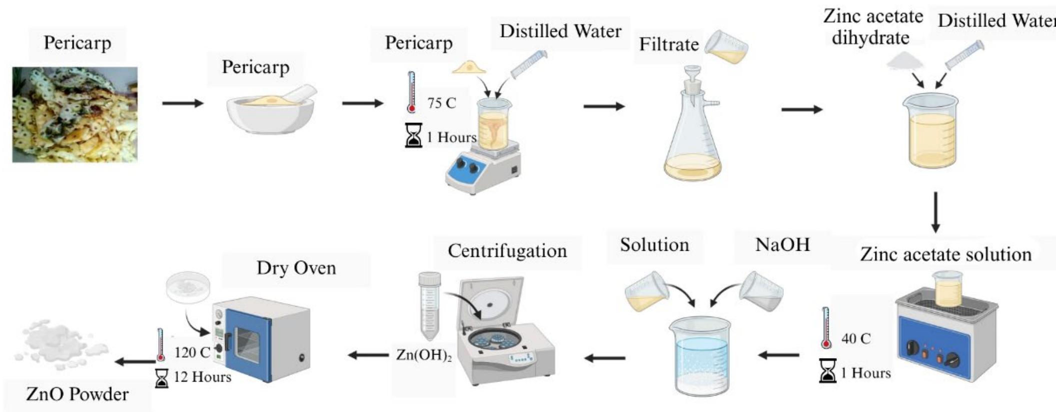

Figure 1. Synthesis procedure of ZnO nanoparticles

$$Zn(CH_3COO)_2 \cdot 2H_2O_{(s)} \rightarrow Zn^{2+}{}_{(aq)} + 2CH_3COO^-{}_{(aq)} + 2H_2O_{(l)} \quad (1)$$

1) Complex formation with phenolic compounds (sonication process 40°C)

$$Zn^{2+}{}_{(aq)} + n\ Phenolics\text{-}OH_{(aq)} \rightleftharpoons [Zn(Phenolate)_n]^{2+}{}_{(aq)} + n\ H^+{}_{(aq)} \quad (2)$$

2) Bioreduction of Zn^{2+} to Zn^0 by pineapple peel extract as a reducing agent (alkaline pH ~10-13)

$$[Zn(Phenolate)_n]^{2+}{}_{(aq)} + Polyphenols_{(aq)} \rightarrow Zn^0{}_{(s)} + Oxidized\ phenolics_{(aq)} \quad (3)$$

The polyphenols from pineapple peel extract act as natural reducing agents, donating electrons (e^-) and protons (H^+) to convert Zn^{2+} ions into nanoscale zinc metal particles (Zn^0). A high pH is required to activate the polyphenols and allow them to act as reducing agents.

3) Addition of NaOH to form $Zn(OH)_2$ in a basic state

$$Zn^0{}_{(s)} + 2NaOH_{(aq)} + \tfrac{1}{2}O_{2\,(g)} \rightarrow Zn(OH)_{2\,(s)} + H_2O_{(l)} + Na^+{}_{(aq)} \quad (4)$$

This stage, after centrifugation, yields $Zn(OH)_2$ solids and a clear supernatant containing Na^+ ions and water, which is then dried.

4) Dehydration of $Zn(OH)_2$ into ZnO nanoparticles during drying

$$Zn(OH)_{2\,(s)} \rightarrow ZnO_{(s)} + H_2O_{(g)} \quad (5)$$

An illustration of the formation of ZnO nanoparticles during the green synthesis process is shown in Figure 2.

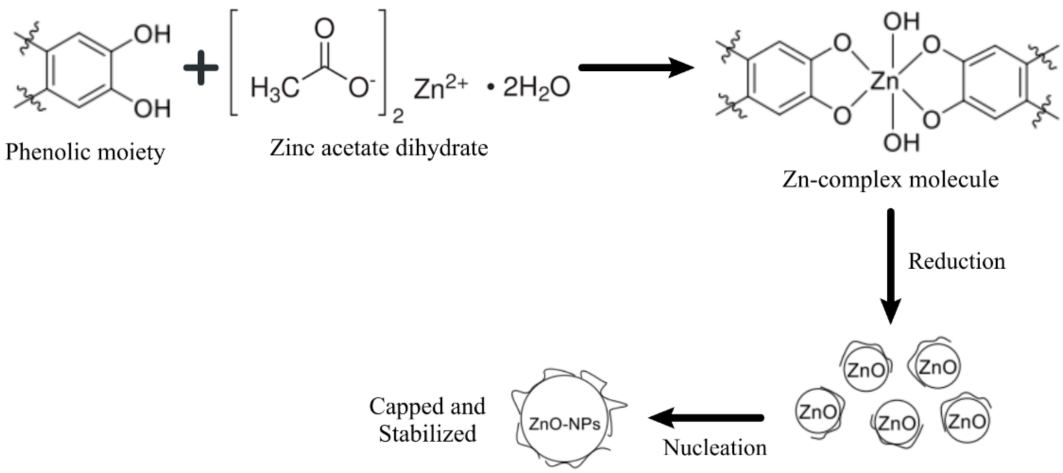

Figure 2. Mechanism of ZnO nanoparticle formation by bioreduction of pineapple peel extract

After the ZnO nanoparticle powder was formed, the fabrication process of the ZnO/Zein nanocomposite was carried out, as shown in Figure 3, which consisted of the following stages. First, a ZnO/Zein mixture was prepared with a 1:2 ratio, which was achieved by dissolving 0.2 g of ZnO into 15 mL of PVA solution. This solution was then stirred using a stirrer at a speed of 500 rpm for 90 min at a temperature of 80°C. The next stage involved dissolving 0.35 g of 1 M NaOH in 95 mL of ethanol, along with 0.4 g of Zein polymer. This mixture was sonicated for 30 min to accelerate the formation of zein aggregates and produce a homogeneous solution. After that, the ZnO solution and zein solution were mixed using a stirrer at a speed of 500 rpm at a temperature of 80°C for 30 min to evaporate the ethanol. Next, the ZnO/Zein mixture was centrifuged at 2500 rpm for 45 min to separate the solid phase from the liquid phase, resulting in a yellow precipitate. The ZnO/Zein solid precipitate was then dried in an oven at 60°C for 6 h. For the ZnO/Zein composition with a ratio of 1:3, the procedure used was the same, using 0.2 g of ZnO and 0.6 g of Zein. In this study, ZnO/Zein compositions of 1:2 and 1:3 were used. These ratios were based on previous studies on Zein-coated ZnO (Naguib et al., 2018), where systems with relatively high Zein content were shown to be able to reduce ZnO aggregation, increase dispersion stability in repeated media and produce more ZnO release, sustaining antibacterial activity.

2.2 Preparation of antibacterial activity test

Antibacterial activity was evaluated using the Kirby-Bauer disc diffusion method. Three sample formulations, namely ZnO nanoparticles, ZnO/Zein (1:2), and ZnO/Zein (1:3) nanocomposites, each at five concentration levels (0.5, 1, 1.5, 2, and 2.5%) were tested against two bacterial strains: *Staphylococcus aureus* (ATCC 25923) and *Streptococcus mutans* (ATCC 25175). A 0.2% chlorhexidine mouthwash solution and distilled water served as positive and negative controls, respectively, for each bacterial strain. Bacterial suspensions with an optical density of 0.1 at a wavelength of 600 nm were prepared, and 100 µL of each suspension was evenly spread onto the surface of Mueller Hinton Agar

(MHA) using a sterile cotton swab. Paper discs impregnated with 30 µL of each test sample were placed onto the inoculated agar surface. The petri dishes were incubated at 35°C for 24 h. The assay was performed in triplicate, and antimicrobial activity was determined by measuring the diameter of the inhibition zone formed around each disc. The stages of the antibacterial test preparation process are illustrated in Figure 4.

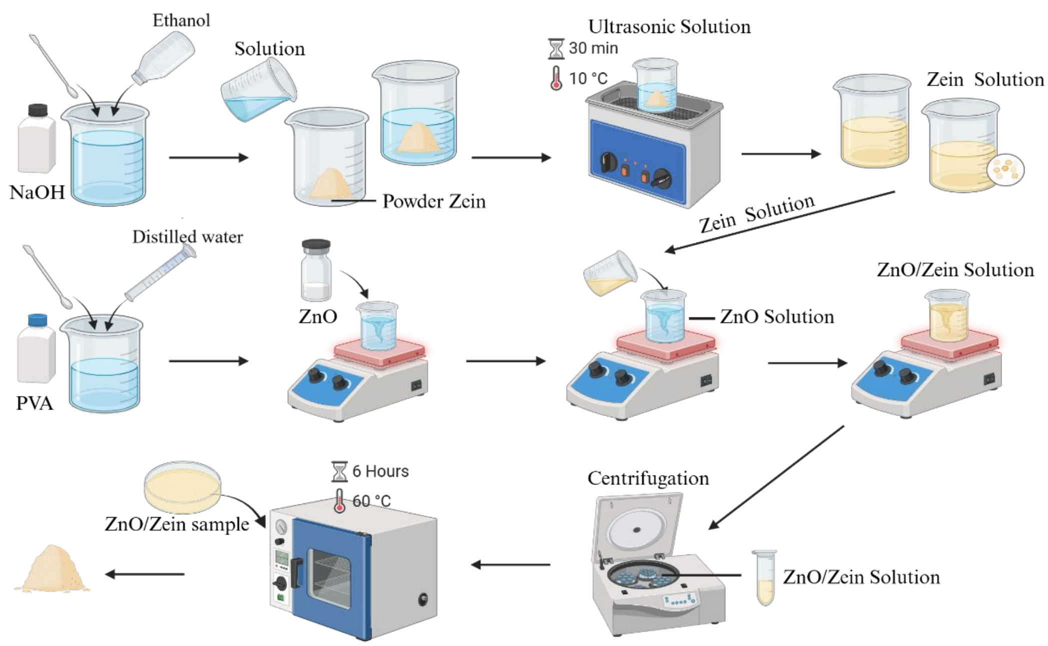

Figure 3. Fabrication procedure of ZnO/Zein nanocomposite

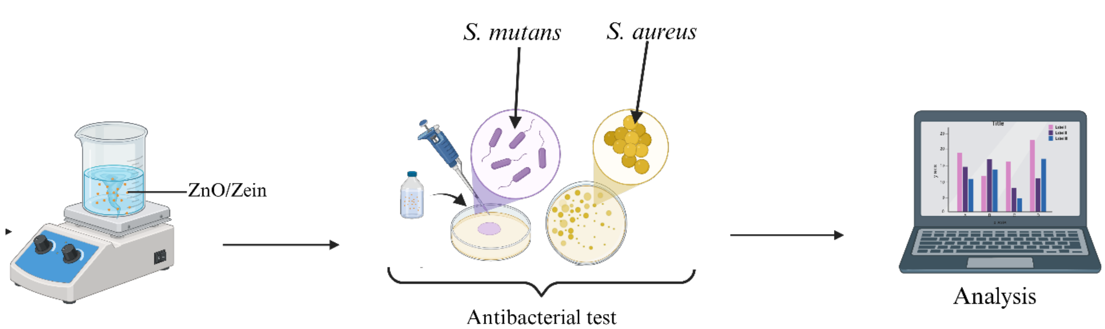

Figure 4. Antibacterial activity process

2.3 Characterization

In this study, the crystal structure characterization of the synthesized samples was carried out using an XRD (X-ray Diffraction) Smartlab Rigaku, supported by High Score Plus software and the powder diffraction file (PDF) database. The test was conducted using a Cu anode radiation source at a voltage of 40 kV, a current of 30 mA, and a Cu K_α wavelength of 1.54 Å, with a Bragg-Brentano optical system. Measurements were carried out at an angle of 5° to 90° with a data collection step of 0.01° per minute. From the results of the XRD test, the diffraction pattern formed was used for phase identification using the Match! Software, and the crystallite size was calculated using Scherrer, according to equation (6), as follows:

$$D = \frac{\lambda K}{\beta \cos\theta} \tag{6}$$

where *D* is the average crystallite size (nm), *K* is a constant (0.94), *λ* is the wavelength of x-rays (0.154 nm), *β* is the FWHM (full width at half maximum) in radians, and *θ* is the diffraction angle in radians. The distance between crystal planes (d_{hkl}) for the wurtzite structure was calculated using the formula according to equation (7) below:

$$\frac{1}{d_{hkl}^2} = \frac{4}{3} \cdot \frac{h^2 + hk + k^2}{a^2} + \frac{l^2}{c^2} \tag{7}$$

where *a* and *c* are the crystal lattice parameters (nm), while *h*, *k*, and *l* are the Miller indices of the crystal plane. The microstrain (*ε*) and dislocation density (*ρ*) in the crystal was determined using the Williamson and Smallman equations according to equations (8) and (9) with *n* (diffraction order) of 1 (Rao et al., 2018; Khier et al., 2021) as follows:

$$\varepsilon = \frac{\beta \ Cos\ \theta}{4} \tag{8}$$

$$\rho = \frac{n}{d_{hkl}^2} \tag{9}$$

Fourier transform infrared (FTIR) testing, using a Shimadzu IR Tracer-100, was conducted in this study to identify the functional groups present in the samples. The test results are presented as absorption peaks in the wavenumber range of 4000 to 500 cm^{-1}. Characterization of the sample surface morphology was performed using a Thermo Fisher Phenom ProX type SEM (scanning electron microscope) with a magnification of up to 30,000 times. From the SEM results, the image of the elements in the sample was analyzed using EDX (energy dispersive X-ray). To determine the grain size distribution, the best image from the SEM results was processed using ImageJ software, considering 100 grains as the analysis data.

3. Results and Discussion

The XRD results of the samples in this study are shown in Figure 5(a). The ZnO/Zein samples of composition (1:2) and (1:3) had the same diffraction peaks as the pure ZnO sample according to the JCPDS (joint committee on powder diffraction standards) standard, File No. 36-1451. The diffraction patterns confirmed the presence of the wurtzite phase with crystal plane orientations of (100), (002), (101), (102), (110), (103), (200), (112), (201). In Figure 5(b), it can be seen that the diffraction peaks in both ZnO/Zein samples exhibit a slight shift and broadening, which can be attributed to the presence of the Zein polymer in the sample structure. The XRD results of the Zein sample showed two diffraction peaks at 2θ angles of 9.96° and 19.73°, with broad, horizontal peak shapes and a wide halo around these angles, indicating the amorphous nature of the polymer (Naguib et al., 2018; Jeong et al., 2025). In the ZnO/Zein compositions (1:2) and (1:3) in Figure 5(a), the Zein peak was not found at these angles. In addition to the presence of the highly crystalline ZnO phase with its dominant high diffraction peak and greater scattering ability that masked the weak Zein diffraction signal, the Zein molecules were dispersed as a thin layer or matrix around the ZnO nanoparticles, so that the size of the neatly arranged Zein domains became very small and the chain arrangement became irregular. As a result, the Zein contribution only appeared as an amorphous background and did not appear as a separate diffraction peak.

In Figure 5(b), it is evident that the ZnO/Zein (1:2) sample exhibited a shift in the diffraction peak towards a larger 2θ angle, indicating a decrease in the interplanar distance. Conversely, in the ZnO/Zein (1:3) sample, there was a shift in the peak to a smaller angle, which indicated an increase in the distance between the crystal planes. The change in the peak to a larger angle was likely caused by the presence of compressive stress in the crystal lattice. Conversely, increasing the polymer content can cause a shift in the peak towards a smaller angle due to tensile strain, thereby increasing the distance between the crystal planes (Indolia & Gaur, 2013). According to Figure 5(b), a diffraction peak shift was observed at an angle of 36.3°, corresponding to a known crystal plane orientation (101). The FWHM of the ZnO/Zein (1:2) and (1:3) samples at that angle were 0.563° (1.768 radians) and 0.526° (1.652 radians), respectively, while the pure ZnO sample was 0.388° (1.218 radians). The difference in FWHM in the three samples affected the crystallite size and dislocation density. According to equation (9), the dislocation densities (ρ) for the ZnO, ZnO/Zein (1:2), and ZnO/Zein (1:3) samples were 9.09×10^{14}, 21.11×10^{14}, and 19.44×10^{14} lines/cm^2, respectively. More details are presented in Table 1. The dislocation density value tended to increase when Zein polymer was added. This indicated the presence of strain and distortion in the ZnO crystal structure, which inhibited the growth of ZnO crystals. However, in the ZnO/Zein composition of 1:3, the dislocation density decreased, and even the crystallite size increased. It is known that the crystallite sizes of ZnO and ZnO/Zein (1:2 and 1:3) are 33.17, 21.77 nm (1:2) and 22.68 nm (1:3). This increase in crystallite size in the ZnO/Zein composition (1:3) was due to the presence of Zein, which actually allowed agglomeration so that Zein was unable to inhibit the growth of ZnO crystals. However, all samples in this study were included in the nanocrystallite category because their sizes were ≤100 nm (Dong et al., 2021). The increase in dislocation density and lattice strain due to the addition of Zein can increase crystal defects and active sites on the ZnO surface, potentially enhancing surface reactivity, Zn^{2+} release, and ROS formation. Thus, structural modifications to the ZnO/Zein nanocomposite were expected to enhance its antibacterial activity and functional performance as a mouthwash.

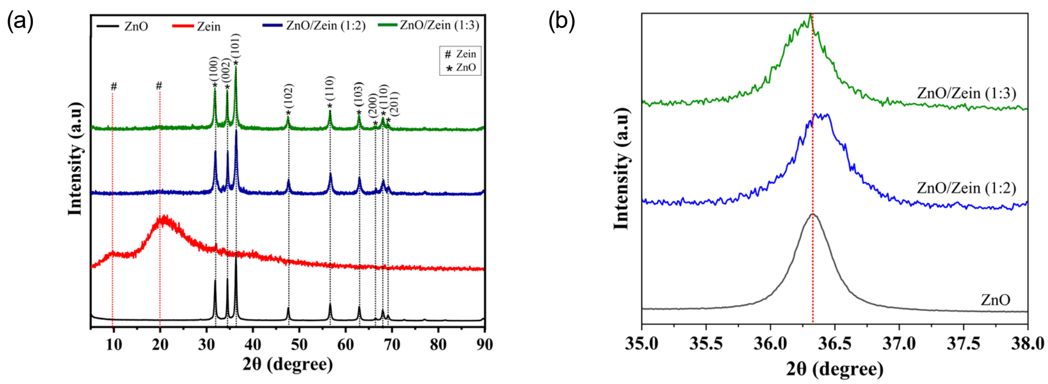

Figure 5. XRD results (a) sample diffraction pattern, (b) magnification of the diffraction peak at the crystal plane orientation (101)

Table 1. XRD spectrum data on zno/zein sample

Sample	Planes (101) 2θ	FWHM (°)	$d_{(101)}$ (nm)	Crystallite size (nm)	Lattice parameters (Å) a=b	c	c/a	ε (x 10^{-3})	(ρ)×10^{14} lines/cm^2
ZnO	36.94	0.38	2.43	33.17	3.175	5.206	1.639	1.692	9.09
ZnO/ Zein (1:2)	36.36	0.56	2.467	21.77	3.235	5.21	1.61	2.456	21.11
ZnO/ Zein (1:3)	36.30	0.52	2.473	22.68	3.243	5.214	1.607	2.294	19.44

The peak shift in the crystal plane orientation (101) presented in Table 1 indicated a strong interaction between the Zein matrix and ZnO. The shift that occurred resulted in an increase in the distance between crystals caused by crystal lattice defects. With increase in the concentration of Zein in ZnO, in the case at the composition of 1: 2 and 1: 3 ZnO/Zein, the c/a value decreased, which indicated a dominant compressive strain along the c-axis due to the interaction of ZnO and Zein, where the presence of Zein causes more defect lines (Khatir & Zak, 2024). Compressive strain increases FWHM and decreases the crystallite size. Although there was a shift in the diffraction peak, there was no significant difference between pure ZnO and the composite with Zein, indicating that the wurtzite structure was still exhibited. The crystal lattice parameters of the wurzite structure, as reported by Rao et al. (2018), show that pure ZnO had a crystal constant (a = b = 3.235 Å, c = 5.213 Å), and the data that had been obtained showed an approach to the value that s not much different.

The FTIR results of ZnO and ZnO/Zein samples at wavenumbers of 4000 to 500 cm^{-1} are shown in Figure 6. The black line, which is that of the ZnO sample, indicated organic compound bonds at wavenumbers 3350 to 865 cm^{-1}. These were attributable to the presence of organic molecules from the pineapple peel extract (used as the bioreductant synthesized via green synthesis of the ZnO nanoparticles) adhering to and functioning as a capping agent on the ZnO surface. Küünal (2022) reported that the main functional groups involved in the reduction of metal ions included hydroxyl, carbonyl, amino, and methoxide groups, which bound to metal ions through electrostatic forces, thereby triggering their reduction. The C-N stretching vibration at 1425 cm^{-1} in the FTIR spectrum was attributed to the amine group in the remaining organic compounds of the bioreductant from pineapple peel extract, which contained free amino acids, and to the presence of the enzyme bromelain, which contributes significantly to the overall protein content (Campos et al., 2020). Sidhu et al. (2022) reported that amino groups in proteins and amino acids played a role in binding to metal surfaces, thereby providing steric hindrance that stabilized nanoparticles and prevented aggregation.

In this study, the authors did not perform separate FTIR or UV-Vis analyses of the pineapple peel extract, as the main focus was on characterizing the resulting ZnO/Zein nanocomposite. The role of pineapple peel extract as a reducing agent and stabilizer has been widely reported. Klinbumrung et al. (2022) and several other studies (Alzura et al., 2025; Rini et al., 2025) on the green synthesis of ZnO from pineapple peel showed that the extract contained phenolic compounds, flavonoids, and the functional groups O–H, C=O, C=C, and C–O, which were confirmed through FTIR analysis. These groups played a role in the process of metal ion reduction and nanoparticle stabilization. Therefore, in this study, we refer to the results of these characterizations and used similar synthesis conditions; assuming that the reduction and stabilization mechanisms of the pineapple peel extract operate similarly, although FTIR/UV–Vis measurements of the pure extract were not explicitly repeated.

The absorption peak of ZnO/Zein in FTIR spectrum was identified at a wavenumber of 3402 cm^{-1}, which indicated an O-H chemical bond, namely the bond between an alcohol and a phenol. The covalent bond C-H or CH_2 was detected at a wavenumber of 2931 cm^{-1}, corresponding to the stretching of the methylene group associated with the organic compound Zein during the formation of the matrix. At wavenumber 1649 cm^{-1}, the ZnO/Zein sample was indicated to have a functional group -C=O (amide bond I) and 1546 cm^{-1}, which is an amide bond II (-NH) in accordance with the results of previous studies detected at 1642 and 1526 cm^{-1} (Schmitz et al., 2020). The C=C vibration, which is characteristic of aromatic rings of Zein, was detected at a wavenumber of 1438 cm^{-1}. The C-O chemical bond, also characteristic of the Zein matrix structure, is identified at 1091 cm^{-1}.

Additionally, the absorption peak at 839 cm^{-1} in the ZnO/Zein sample indicates a C-N chemical bond related to the aliphatic amine group. It suggests an interaction between ZnO and Zein, which was identified in previous studies in the 1000-600 cm^{-1} region (Ayazi et al., 2024). The presence of the ZnO/Zein composite sample is observed at the absorption peak of 555 cm^{-1}, corresponding to the Zn-O functional group. This was in agreement with Hassanein et al. (2021), who reported it at 573 cm^{-1}. The absorption peaks for each sample are presented in Table 2.

The morphology of the ZnO/Zein sample obtained from SEM-EDX characterization is presented in Figure 7, with a magnification of 30,000 times. The ZnO nanoparticles in Figure 7(a) showed agglomeration, which was indicated by the presence of gaps and uneven particle dispersion, which likely affected their dimensions. The EDX results on the sample showed that the composition of O and Zn elements was 14.70% and 85.30%, respectively. The presence of the N element in the ZnO nanoparticle sample was not detected in the EDX results, even though the FTIR spectrum (Figure 6) indicated C-N bond vibrations from the amino groups of organic compounds present in pineapple peel extract. The amino groups in this protein were weakly adsorbed to the ZnO surface, providing steric hindrance to stabilize the nanoparticles (Sidhu et al., 2022). This superficial adsorption was detected as a C-N peak in the FTIR, but the very low N content did not reach the detection limit of SEM-EDX due to the instrument's limited sensitivity for light elements (Jayachandran et al., 2021; MacArthur et al., 2021).

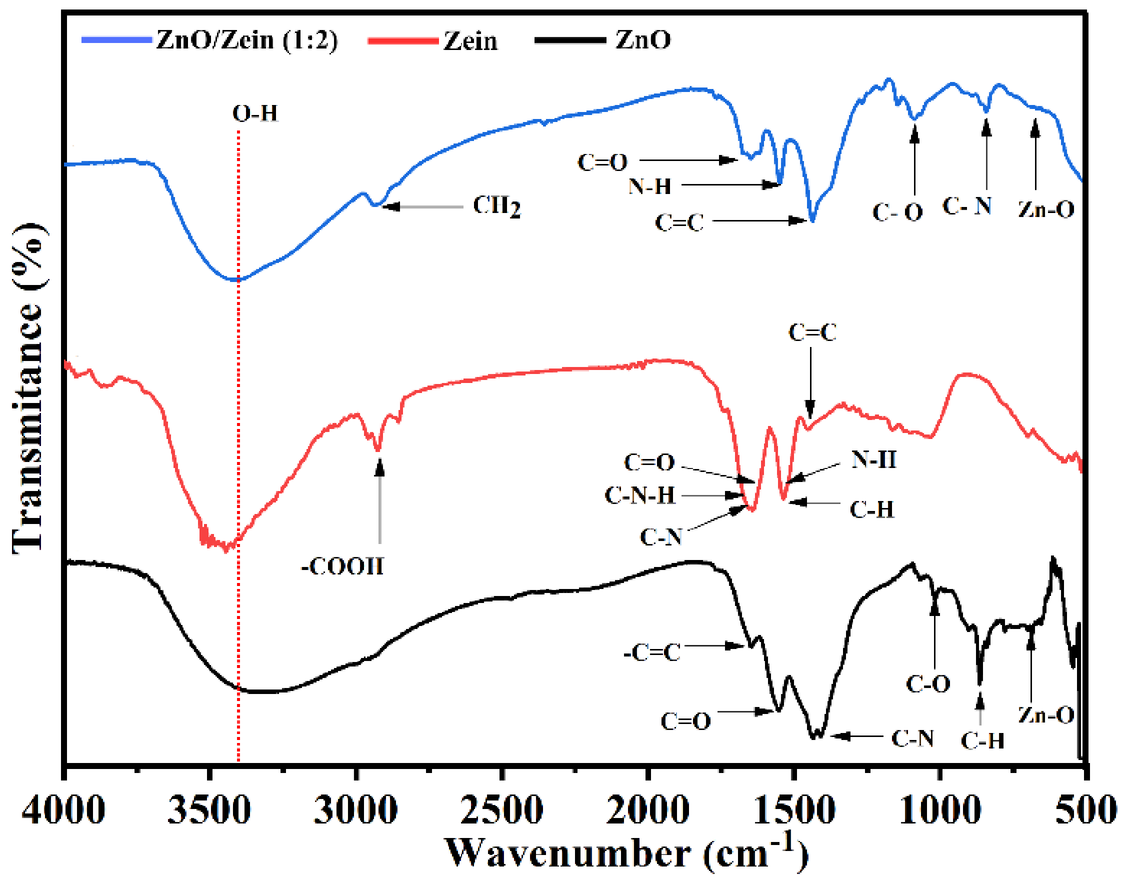

Figure 6. FTIR spectra of the samples

Table 2. Absorption peaks of samples resulting from FTIR characterization

Sample	Wavenumber (cm^{-1})		Types of Bonds
	Experiment	Reference	
ZnO	3350	3435 (El-Khawaga et al., 2025)	-O-H
	1652	1631 (Oktavia & Rohmawati, 2022)	-C=C
	1558	1549 (Rohmawati et al., 2024a)	C=O
	1425	1403 (Abdelbaky et al., 2022)	C-N
	1074	1072 (Abdelbaky et al., 2022)	C-O
	865	875 (Hamouda et al., 2023)	C-H Stretching Vibrations
	779, 688, 554	782, 688, 548 (Rohmawati et al., 2024a)	Zn-O
Zein	3435	3310 (Gonçalves et al., 2020)	O-H bond
	2931	2926 (Rohmawati et al., 2024b)	Stretching N-H
	1645	1650 (Batool et al., 2022)	Stretching C=O (amide I bond)
	1541	1510 (Batool et al., 2022)	Vibration N-H and stretching C-H (amide bond II)
	1450	1400 (Ranimol et al., 2021)	C=C aromatic stretching
	1031	1034 (Gonçalves et al., 2020)	Stretching C-O
ZnO/Zein	3402	3400 (Naguib et al., 2018)	O-H bond
	2931	2954 (Ayazi et al., 2024)	Stretching vibration CH_2
	1649	1642 (Schmitz et al., 2020)	-C=O Amide I bond
	1546	1526 (Schmitz et al., 2020)	-NH Amide Bond II
	1438	1453 (Rohmawati et al., 2024a)	Vibration C=C
	1091	1076 (Hassanein et al., 2021)	C-O stretching
	839	600-1000 (Ayazi et al., 2024)	Vibration of alkene group C-N
	555	573 (Hassanein et al., 2021)	Zn-O

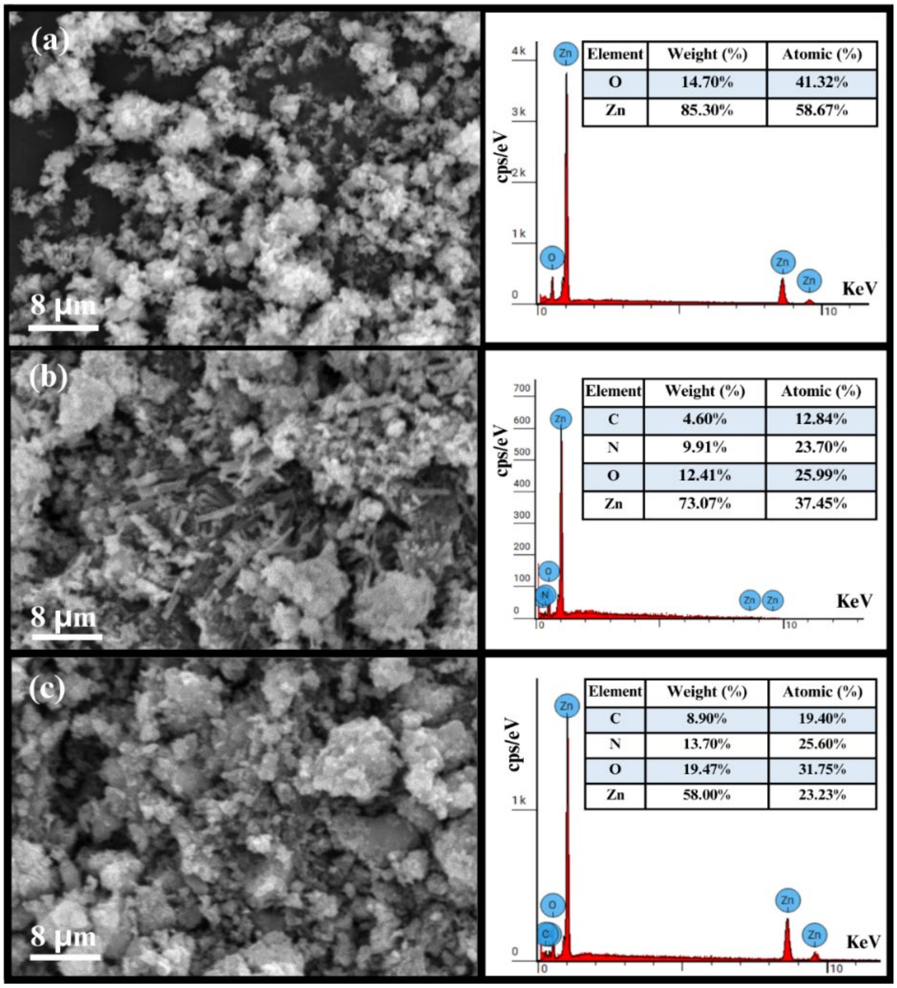

Figure 7. SEM-EDX results (a) ZnO; (b) ZnO/Zein 1:2; (c) ZnO/zein 1:3

The morphological structure of the ZnO/Zein (1:2) nanocomposite in Figure 7 (b-c) showed ZnO nanoparticles evenly dispersed on the Zein surface, with the identified EDX results being C, N, O, and Zn elements, which had elemental weights of 4.60%, 9.91%, 12.41% and 73.07%, respectively. In comparison, the ZnO/Zein (1:3) sample identified similar elements with elemental weights of 8.90%, 13.70%, 19.47%, and 58.00%, respectively. The natural protein properties of Zein can form a protective layer on the ZnO surface, thereby reducing direct interactions between ZnO particles, which can cause aggregation (Pascoli et al., 2018). Zein can play a role in preventing aggregation in ZnO, thus maintaining its nanoscale size (Naguib et al., 2018).

The results for average particle size using ImageJ are shown in Figure 8, which considered 100 grains in each sample. The average grain distribution in the ZnO sample was 54.93 nm, while the ZnO/Zein nanocomposites with compositions of 1:2 and 1:3 had grain sizes of 36.48 nm and 45.37 nm, respectively. Particles with sizes between 1 and 100 nm are referred to as nanoparticles or nanocomposites (Donough et al., 2024).

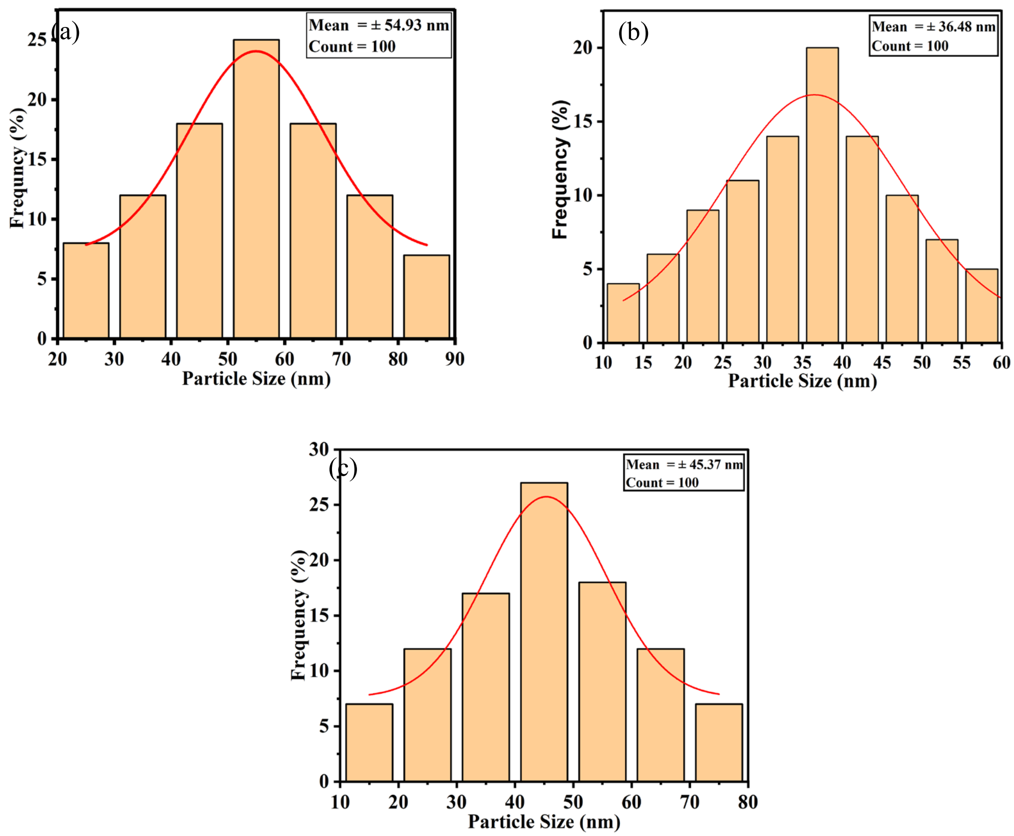

Figure 8. Average particle size distribution (a) ZnO; (b) ZnO/Zein 1:2; (c) ZnO/zein 1:3

Antibacterial activity against *S. aureus* and *S. mutans* bacteria was conducted using the disc diffusion method. The test was performed with 0.5%, 1%, 1.5%, 2% and 2.5% solutions of the ZnO nanoparticle samples and the ZnO/Zein 1:2 and 1:3 samples. A chlorhexidine 0.2% mouthwash solution served as positive control (+) and distilled water served as negative control (-). The results of the antibacterial test were presented in the form of qualitative data, with concentrations of 0.5%, 1%, 1.5%, 2%, and 2.5% marked by clear zones, as shown in Figures 9 and 10.

Differences in the size of the clear zone are visible in Figure 9 for *S. aureus* and in Figure 10 for *S. mutans*. The inhibition zone of *S. aureus* bacteria from ZnO samples and ZnO/Zein compositions of 1:2 and 1:3 appeared larger than that of *S. mutans*. Although the cell walls of *S. aureus* bacteria are thicker (~30 nm peptidoglycan), the absence of an outer membrane allows ZnO nanoparticles to generate ROS that more effectively attack the peptidoglycan and plasma membrane (Abebe et al., 2020; Emami-Karvani & Chehrazi, 2012). Besides that, *S. aureus* bacteria are more sensitive to ZnO because their peptidoglycans are more porous with natural hydrolases that form gaps (Salamaga et al., 2021; Wang et al., 2022). In contrast, *S. mutans* bacteria are more resistant due to their tendency to form biofilms with strong exopolysaccharides, which hinder nanoparticle penetration (Tiwari et al., 2018; Babayevska et al., 2022). More details regarding the results of the inhibition zone diameter measurements are shown in Table 3. Inhibition zone diameter data (mm) are in the form of mean±SD (repetition, n = 3). The effects of sample types such as control (+), ZnO/Zein (1:2), ZnO/Zein (1:3), and concentrations ranging from zero to 2.5%, on the inhibition zone were analyzed using two-way ANOVA, which was then followed by further Tukey HSD tests for comparisons between samples at each concentration. A p-value < 0.05 was considered statistically significant.

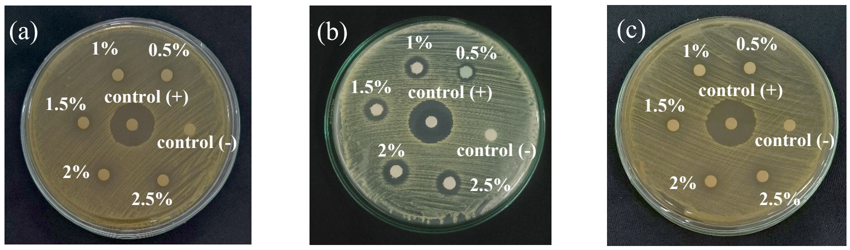

Figure 9. Antibacterial activity test results against *S. aureus* (a) ZnO, (b) ZnO/Zein (1:2), (c) ZnO/Zein (1:3)

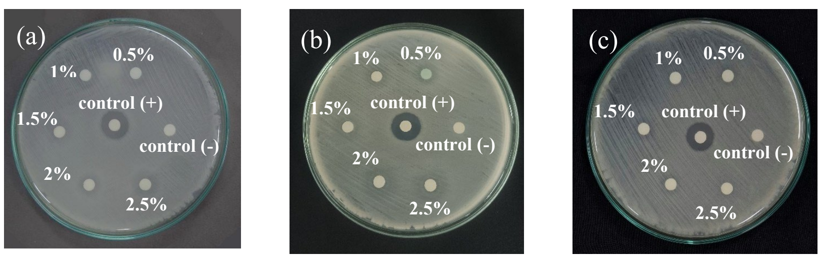

Figure 10. Antibacterial activity test results against *S. mutans* (a) ZnO, (b) ZnO/Zein (1:2), (c) ZnO/Zein (1:3)

In Table 3, the diameter of the inhibition zones of ZnO, ZnO/Zein (1:2), and ZnO/Zein (1:3) against *S. aureus* and *S. mutans* indicates the ability of each sample to inhibit bacterial growth surrounding the sample well, with larger zones reflecting greater antibacterial potency. The antibacterial activity of the three formulations was lower than that of 0.2% chlorhexidine mouthwash (positive control) because the test in this study used only the ZnO/Zein solution in distilled water without other mouthwash additives. According to the two-way ANOVA (Table 4), concentration had a highly significant effect on inhibition zone diameter against *S. aureus* ($F = 13.10$, $p<0.001$), while sample type alone did not show a significant effect ($F = 3.30$, $p = 0.051$). For *S. mutans*, sample type had a highly significant effect ($F = 6.86$, $p = 0.004$), whereas concentration alone did not reach statistical significance ($F = 2.58$, $p = 0.058$). However, the interaction between sample type and concentration was significant for *S. aureus* ($F = 2.45$, $p = 0.036$) and highly significant for S. mutans ($F = 4.52$, $p = 0.001$), indicating that the antibacterial response of each sample type was differentially influenced by concentration.

Table 3. Inhibition zone values of samples against *S. aureus* and *S. mutans* bacteria (mean±SD) and Tukey group

Microorganism	Concentration (%)	Sample	Inhibition Zone Diameter (mm, mean±SD)	Tukey Group*
S. aureus	0	Control (+) (0.2% chlorhexidine)	22.30±0.00	-
	0.5	ZnO	6.53±0.55	a
		ZnO/Zein (1:2)	7.10±0.26	a
		ZnO/Zein (1:3)	7.17±1.07	a
	1	ZnO	8.17±0.64	a
		ZnO/Zein (1:2)	8.30±0.53	a
		ZnO/Zein (1:3)	7.60±1.01	a
	1.5	ZnO	9.07±0.25	a
		ZnO/Zein (1:2)	8.43±0.32	a
		ZnO/Zein (1:3)	7.97±0.21	b
	2	ZnO	10.90±1.56	a
		ZnO/Zein (1:2)	9.00±0.36	a
		ZnO/Zein (1:3)	8.30±0.87	a
	2.5	ZnO	8.50±0.17	a
		ZnO/Zein (1:2)	9.40±0.26	a
		ZnO/Zein (1:3)	8.63±1.44	a
S. mutans	0	Control (+) (0.2% chlorhexidine)	14.80±0.00	-
	0.5	ZnO	8.13±0.71	a
		ZnO/Zein (1:2)	5.53±0.06	b
		ZnO/Zein (1:3)	5.53±0.06	b
	1	ZnO	6.87±0.60	a
		ZnO/Zein (1:2)	5.73±0.06	b
		ZnO/Zein (1:3)	5.73±0.06	b
	1.5	ZnO	6.67±0.83	a
		ZnO/Zein (1:2)	5.73±0.12	a
		ZnO/Zein (1:3)	5.73±0.12	a
	2	ZnO	6.40±0.17	a
		ZnO/Zein (1:2)	6.47±0.98	a
		ZnO/Zein (1:3)	6.47±0.98	a
	2.5	ZnO	6.27±0.40	a
		ZnO/Zein (1:2)	7.20±1.04	a
		ZnO/Zein (1:3)	7.20±1.04	a

*Different letters within the same concentration level indicate significant differences among sample formulation ($p<0.05$, Tukey HSD test)

Table 4. Two-way ANOVA results for the effect of sample type and concentration on inhibition zone diameter against *S. aureus* and S. *mutans*

Bacterium	Source of Variation	df	SS	MS	F	p-value	Sig.
S. aureus	Sample type	2	3.94	1.97	3.30	0.051	ns
	Concentration	4	31.32	7.83	13.10	<0.001	**
	Type × Concentration	8	11.72	1.47	2.45	0.036	*
	Residual	30	17.93	0.598	-	-	-
S. mutans	Sample type	2	5.38	2.69	6.86	0.004	**
	Concentration	4	4.04	1.01	2.58	0.058	ns
	Type × Concentration	8	14.20	1.77	4.52	0.001	**
	Residual	30	11.76	0.392	-	-	-

**p<0.01 (highly significant); *0.01≤p<0.05 (significant); ns = not significant (p≥0.05); SS = sum of squares; MS = mean square; df = degrees of freedom; F = ratio of MS (treatment) to MS (residual)

At a concentration of 2% (Table 3), ZnO nanoparticles produced the largest inhibition zone against *S. aureus* bacteria (10.90±1.56 mm), followed by ZnO/Zein (1:2) (9.00±0.36 mm) and ZnO/Zein (1:3) (8.30±0.87 mm). Although the mean values differed numerically, Tukey HSD post hoc analysis indicated no statistically significant differences among the three formulations at this concentration ($p>0.05$), likely due to the relatively high variability observed in the ZnO replicates (SD = 1.56 mm). It suggests that at 2% concentration, the antibacterial performance of ZnO/Zein nanocomposites was comparable to that of ZnO nanoparticles alone against *S. aureus*. The inhibition zones produced by all tested formulations were considerably lower than that of the 0.2% chlorhexidine positive control (22.30 mm for *S. aureus* and 14.80 mm for *S. mutans*). It is expected that chlorhexidine is a broad-spectrum antiseptic with multiple mechanisms of action and enhanced membrane permeability (Deus & Ouanounou, 2022). In contrast, the test formulations consisted solely of ZnO or ZnO/Zein dispersed in distilled water without additional surfactants or penetration enhancers. Nevertheless, the antibacterial activity demonstrated by ZnO/Zein nanocomposites at concentrations ≥1.5% is considered promising for further formulation development into a complete mouthwash product (Chang et al., 2024). The higher inhibition zones observed for pure ZnO nanoparticles at concentrations 2% compared to ZnO/Zein nanocomposites can be attributed to the absence of a polymeric matrix, which allows Zn^{2+} ions and ROS to diffuse more freely and rapidly into the agar medium (Naqvi et al., 2019). In contrast, the incorporation of Zein polymer may initially retard Zn^{2+} ion release due to its hydrophobic nature, which tends to form a compact layer around the nanoparticles, thereby acting as a diffusion barrier (Naguib et al., 2021). However, at a concentration of 2.5% ZnO, the inhibition zone against *S. aureus* bacteria actually decreased to 8.50±0.17 mm compared to 10.90±1.56 mm at 2%. This was probably caused by the aggregation of ZnO particles, forming larger particle sizes. As a result, the available active area was reduced, weakening the interaction between ZnO and bacteria. This condition inhibited the diffusion process of Zn^{2+} ions into the agar medium, slowing the release of these ions, and ultimately reducing the antibacterial effectiveness at that concentration.

At a concentration of 2.5%, ZnO/Zein (1:2) produced the largest inhibition zone against *S. aureus* bacteria (9.40±0.26 mm), followed by ZnO/Zein (1:3) (8.63±1.44 mm) and ZnO nanoparticles (8.50±0.17 mm) (Table 3). Tukey HSD post hoc analysis revealed no statistically significant differences among the three formulations at this concentration ($p>0.05$), likely due to high variability in ZnO/Zein (1:3) replicates (SD = 1.44 mm) and the relatively small differences in mean values, indicating comparable antibacterial performace across all formulations at this concentration. The relatively higher inhibition zone of ZnO/Zein (1:2) may be attributed to the role of Zein in preventing nanoparticle agglomeration, thereby maintaining a larger effective surface area and sustaining Zn^{2+} ion release. In contrast, the ZnO.Zein (1:3) formulation, which contains a higher Zein content, may form a thicker polymeric layer, resulting in more restricted Zn^{2+} release and hindered ROS diffusion, which may partially reduce its antibacterial efficacy to ZnO/Zein (1:2). The inhibition zones of ZnO nanoparticles at 0.5% and 1% against *S. aureus* (6.53±0.55 mm and 8.17±0.64 mm, respectively) were higher than those reported by El-Masry et al. (2022), who observed inhibition zones of 5 mm and 6 mm at comparable ZnO concentrations. This difference may be attributed to variations in nanoparticles size and synthesis method, as smaller nanoparticles with greater surface area-to-volume ratios generally exhibit enhanced antibacterial activity (Naqvi et al., 2019).

Similarly, at a concentration of 0.5%, ZnO nanoparticles produced a significantly larger inhibition zone against *S. mutans* (8.13±0.71 mm) compared to both ZnO/Zein (1:2) and ZnO/Zein (1:3) (5.53±0.06 mm each, $p<0.05$ Tukey HSD). At this concentration, ZnO was well dispersed, allowing the metal ions in the sample to penetrate the *S. mutans* biofilm optimally.

With increasing concentration from 0.5 to 2.5%, both ZnO/Zein (1:2) and ZnO/Zein (1:3) exhibited a concentration-dependent increase in inhibition zone diameter against *S. mutans*, ranging from 5.53±0.06 mm to 7.20±1.04 mm. Notably, both formulations produced identical inhibition zone values across all tested concentrations, suggesting that the difference in ZnO:Zein ratio (1:2 vs. 1:3) did not affect antibacterial activity against *S. mutans* under the tested conditions. This finding indicates that within the studied ratio range, antibacterial efficacy was predominantly determined by the total ZnO content rather than the Zein proportion, and the variation in Zein content between the two formulations was insufficient to produce a detectable difference in Zn^{2+} ion release rate within 24 h (Naguib et al., 2018). To further characterize the antibacterial potential of these formulations, determination of the Minimum Inhibitory Concentration (MIC) using the broth microdilution method is recommended as a complementary approach to provide quantitative data on the lowest effective concentration required to inhibit bacterial growth (Alqaffaf et al., 2026). At a concentration of 2.5%, ZnO/Zein (1:2) and ZnO/Zein (1:3) produced larger inhibition zones (7.20±1.04 mm each) against *S. mutans* compared to ZnO nanoparticles alone (6.27±0.40 mm). However, Tukey HSD post hoc analysis indicated no statistically significant differences among the three formulations at this concentration ($p>0.05$), likely due to the high variability in ZnO/Zein replicates (SD = 1.04 mm) and the small absolute differences in mean values. This observation suggests that Zein plays an important role in maintaining ZnO nanoparticle stability at higher concentrations by preventing agglomeration, thereby preserving a larger effective surface area for Zn^{2+} ion release and bacterial interaction (Naguib et al., 2018).

Based on the antibacterial test results, ZnO/Zein nanocomposites demonstrated potential as antibacterial materials for oral health applications, with mean inhibition zone diameters ranging from 7.10 to 9.40 mm against *S. aureus* and from 5.53 to 7.20 mm against *S. mutans*, which fall within the moderate antibacterial activity category (5-10 mm) according to Davis & Stout (1971). Although the inhibition zone diameters of ZnO/Zein nanocomposites were lower than those of pure ZnO, two-way ANOVA (Table 4), the results revealed that concentration had a highly significant effect on inhibition zone diameter against *S. aureus* ($F=13.10$, $p<0.001$). In contrast, the interaction between sample type and concentration was significant for both *S. aureus* ($p = 0.036$) and *S. mutans* ($p = 0.001$). This concentration-dependent response was particularly evident in ZnO/Zein nanocomposites, which showed a consistent increase in inhibition zone diameter from 7.10 to 9.40 mm (*S. aureus*) and 5.53 to 7.20 mm (*S. mutans*) with increasing concentration, suggesting that the Zein matrix stabilizes ZnO nanoparticle dispersion and supports sustained antibacterial activity across the tested concentration range. This study did not evaluate the long-term colloidal stability of ZnO/Zein nanocomposites in aqueous solution. However, the inhibition zone data in Table 3 indirectly reflect short-term functional stability during the 24-hour incubation period, as both ZnO/Zein (1:2) and ZnO/Zein (1:3) maintained a consistent concentration-dependent increase in inhibition zone diameter against *S. aureus* (7.10-9.40 mm and 7.17-8.63 mm, respectively) and *S. mutans* (5.53-7.20 mm for both formulations) with increasing concentration. In contrast, pure ZnO showed a declining trend against *S. mutans* from 8.13 mm at 0.5% to 6.27 mm at 2.5%, with a notable decrease beginning at 1.0% concentration (6.87 mm), which may be attributed to nanoparticle aggregation at higher concentrations, as previously reported for uncoated ZnO nanoparticles (Sirelkhatim et al., 2015). This result is in line with previous research reported by Ma et al. (2019) on the ZnO-protein casein system in the form of nanocomposites, which showed that ZnO in a protein matrix increased colloid stability compared to pure ZnO, and, in that study, the emulsion was stable for up to 6 months, and it continued to reduce the aggregation of ZnO.

The quality of pineapple peel and its extract as bioreductants and capping agents greatly determined the size, morphology, and stability of ZnO nanoparticles produced in the green synthesis process. If developed on an industrial scale, then the quality control of pineapple peel needs to be carried out by establishing botanical specifications, ensuring the fruit comes from controlled sources and regulating post-harvest handling conditions (washing, peeling methods and cold storage time limits before extraction). These procedures need to be accompanied by water content and contaminant tests for pesticide residues, mycotoxins and microbial contamination, which need to be conducted according to material and herbal quality guidelines. For the extraction process, it is necessary to standardize factors such as solvent type, solid-to-solvent ratio, time, and temperature, and to characterize the extracts based on reducing compound content and chromatographic profiles to ensure consistency between batches.

4. Conclusions

In this study, ZnO nanoparticles were successfully combined with Zein through a mixing method, resulting in ZnO/Zein nanocomposites with compositions of 1:2 and 1:3. Both nanocomposites exhibited a wurtzite phase crystal structure, as well as a shift in diffraction peaks, indicating a strong interaction between the Zein and the ZnO matrix. Zein was also shown to be able to prevent ZnO particle agglomeration, which was seen from the decrease in the average grain size: pure ZnO measured 54.93 nm, while ZnO/Zein 1:2 and 1:3 measured 36.48 nm and 45.37 nm, respectively. The antibacterial effectiveness against *S. aureus* and *S. mutans* depended on the concentration of the nanocomposite. At a concentration of 2.5%, ZnO/Zein 1:2 showed the largest inhibition zone against *S. aureus*, which was 9.40±0.26 mm, surpassing ZnO/Zein 1:3 (8.63±1.44 mm) and pure ZnO (8.50±0.17 mm). Meanwhile, against *S. mutans*, ZnO/Zein nanocomposites at a 1:2 and 1:3 ratio showed a consistent increase in inhibition zone diameter from 5.53 mm at 0.5% to 7.20 mm at 2.5%. Although the inhibition zones of ZnO/Zein nanocomposites were not always higher than pure ZnO at certain concentrations, their concentration-dependent antibacterial response was more consistent, suggesting better dispersion stability of ZnO within the Zein matrix. Due to these properties, ZnO/Zein nanocomposites have potential as additional ingredients in mouthwash formulations.

5. Acknowledgements

This research was made possible with the assistance of the ZnO nano research team and funding support from the Institute for Research and Community Service (LPPM) of Universitas Negeri Surabaya, based on research contract number B/33130/UN38.III.1/LK. 04.00/2025 and Decree of the Rector of Universitas Negeri Surabaya Number 520/UN38/ HK/2025.

6. Authors' Contributions

Woro Setyarsih: Conceptualization, writing-original draft, writing-review and editing. Mohamad Wafiq Nafii Alfan: Resources, writing-review and editing. Fitriana: Investigation and methodology, writing-review and editing. Tukiran: Coordinated research, writing-review and editing. Erlix Rakhmad Purnama: Resources, validation, writing-review and editing. Prima Nerito: investigation and methodology, writing-review and editing. R Sabda

Alam: Investigation, writing-review and editing. Lydia Rohmawati: Analyzed data, writing-original draft, writing-review and editing.

ORCID
Woro Setyarsih https://orcid.org/0000-0001-8344-2768
Fitriana https://orcid.org/0009-0004-1888-813X
Tukiran https://orcid.org/0000-0001-6613-128X
Erlix Rakhmad Purnama https://orcid.org/0000-0002-4066-3357
Prima Nerito https://orcid.org/0009-0003-6667-1915
Lydia Rohmawati https://orcid.org/0000-0002-0047-3487

7. Conflicts of Interest

The authors declare no conflict of interest.

References

Abdelbaky, A. S., El-Mageed, T. A. A., Babalghith, A. O., Selim, S., & Mohamed, A. M. H. A. (2022). Green synthesis and characterization of ZnO nanoparticles using *Pelargonium odoratissimum* (L.) aqueous leaf extract and their antioxidant, antibacterial and anti-inflammatory activities. *Antioxidants*, *11*(8), Article 1444. https://doi.org/10.3390/antiox11081444

Abebe, B., Zereffa, E. A., Tadesse, A., & Murthy, H. C. A. (2020). A review on enhancing the antibacterial activity of ZnO: Mechanisms and microscopic investigation. *Nanoscale Research Letters, 15*(1), Article 190. https://doi.org/10.1186/s11671-020-03418-6

Afra, S. M., & Modaresi, F. (2017). The use of synergistically antiplaque nanoparticles in treating dental caries. *Journal of Dental Health, Oral Disorders and Therapy*, *6*(5), 144-149. https://doi.org/10.15406/jdhodt.2017.06.00214

Almoudi, M. M., Hussein, A. S., Hassan, M. I. A., & Zain, N. M. (2018). A systematic review on antibacterial activity of zinc against Streptococcus mutans. *Saudi Dental Journal*, *30*(4), 283-291. https://doi.org/10.1016/j.sdentj.2018.06.003

Alqaffaf, D., Atoom, A. M., Huwaij, R. A., Abusalah, M. A. H. A., Alzubi, B. T., Al-Kaabneh, A., Abusalah, M. A. H. A., & Sughayer, M. A. (2026). Analysis of the antimicrobial activity of zinc oxide nanoparticles against drug-resistant bacteria and their applications in the disinfection process. *PLoS ONE*, *21*(2), Article e0340470. https://doi.org/10.1371/journal.pone.0340470

Alzura, S. P., Saraswaty, V., Ishmayana, S., Budiman, Y. P., Eddy, D. R., Aji, E. S., Ratnaningrum, D., Endah, E. S., Meirinawati, H., & Setiyanto, H. (2025). Synthesis and characterization of zinc oxide nanoparticles-carbon composite derived from pineapple peel wastes for adsorption of methylene blue from solution and photocatalytic activity. *Case Studies in Chemical and Environmental Engineering*, *11*, Article 101113. https://doi.org/10.1016/j.cscee.2025.101113

Ayazi, D., Zandi, M., Ganjloo, A., & Dardmeh, N. (2024). Bioactive electrospun zein fibers integrated with ZnO nanoparticles: In vitro investigations. *Food Bioscience*, *62*, Article 105343. https://doi.org/10.1016/j.fbio.2024.105343

Babayevska, N., Przysiecka, Ł., Iatsunskyi, I., Nowaczyk, G., Jarek, M., Janiszewska, E., & Jurga, S. (2022). ZnO size and shape effect on antibacterial activity and cytotoxicity profile. *Scientific Reports*, *12*, Article 8148. https://doi.org/10.1038/s41598-022-12134-3

Batool, S. A., Ahmad, K., Irfan, M., & Ur Rehman, M. A. (2022). Zn–Mn-doped mesoporous bioactive glass nanoparticle-loaded zein coatings for bioactive and antibacterial orthopedic implants. *Journal of Functional Biomaterials*, *13*(3), Article 97. https://doi.org/10.3390/jfb13030097

Bortoletto-Santos, R., Plotegher, F., Roncato, V., Majaron, R. F., Majaron, V. F., Polito, W. L., & Ribeiro, C. (2018). Strategy for multinutrient application in integrated granules using zein as a coating layer. *Journal of Agricultural and Food Chemistry*, *66*(37), 9582-9587. https://doi.org/10.1021/acs.jafc.8b01319

Brookes, Z., Teoh, L., Cieplik, F., & Kumar, P. (2023). Mouthwash effects on the oral microbiome: Are they good, bad, or balanced? *International Dental Journal*, *73*(Suppl 2), S74-S81. https://doi.org/10.1016/j.identj.2023.08.010

Brunello, G., Becker, K., Scotti, L., Drescher, D., Becker, J., & John, G. (2022). Effect of three chlorhexidine-based mouthwashes on human gingival fibroblasts: An in vitro study. *Applied Sciences*, *12*(5), Article 2417. https://doi.org/10.3390/app12052417

Campos, D. A., Ribeiro, T. B., Teixeira, J. A., Pastrana, L., & Pintado, M. M. (2020). Integral valorization of pineapple (*Ananas comosus* L.) by-products through a green chemistry approach towards added value ingredients. *Foods*, *9*(1), Article 60. https://doi.org/10.3390/foods9010060

Cao, Y., Chen, T. T., Wang, W., Chen, M., & Wang, H. J. (2017). Construction and functional assessment of zein thin film incorporating spindle-like ZnO crystals. *RSC Advances*, *7*(4), 2180-2185. https://doi.org/10.1039/c6ra25290g

Carrouel, F., Viennot, S., Ottolenghi, L., Gaillard, C., & Bourgeois, D. (2020). Nanoparticles as anti-microbial, anti-inflammatory, and remineralizing agents in oral care cosmetics: A review of the current situation. *Nanomaterials*, *10*(1), Article 140. https://doi.org/10.3390/nano10010140

Chang, L., Gan, R., Huang, X., Zheng, D., Su, C., Lu, Y., & Feng, Y. (2024). Application of novel nanomaterials with dual functions of antimicrobial and remineralization in mouthwashes. *Scientific Reports*, *14*(1), Article 29027. https://doi.org/10.1038/s41598-024-80703-9

Davis, W. W., & Stout, T. R. (1971). Disc plate method of microbiological antibiotic assay I. Factors influencing variability and error. *Applied Microbiology*, *22*(4), 659-665. https://doi.org/10.1128/am.22.4.659-665.1971

de Almeida Campos, L., Neto, A. F. S., Noronha, M. C. S., de Lima, M. F., Cavalcanti, I. M. C., & Santos-Magalhães, N. S. (2023). Zein nanoparticles for drug delivery: Preparation methods and biological applications. *International Journal of Pharmaceutics*, *635*, Article 122754. https://doi.org/10.1016/j.ijpharm.2023.122754

Deus, F. P., & Ouanounou, A. (2022). Chlorhexidine in dentistry: Pharmacology, uses, and adverse effects. *International Dental Journal*, *72*(3), 269-277. https://doi.org/10.1016/j.identj.2022.01.005

Dong, Y., Yang, H., Zhang, L., Li, X., Ding, D., Wang, X., Li, J., Li, J., & Chen, I.-W. (2021). Ultra-uniform nanocrystalline materials via two-step sintering. *Advanced Functional Materials*, *31*(1), Article 2007750. https://doi.org/10.1002/adfm.202007750

Donough, N., Wepener, V., & Botha, T. L. (2024). Sizes, shapes, and types of nanomaterials. *Frontiers for Young Minds*, *12*, Article 1356284 https://doi.org/10.3389/frym.2024.1356284

El-Khawaga, A. M., Elsayed, M. A., Gobara, M., Suliman, A. A., Hashem, A. H., Zaher, A. A., Mohsen, M., & Salem, S. S. (2025). Green synthesized ZnO nanoparticles by *Saccharomyces cerevisiae* and their antibacterial activity and photocatalytic degradation. *Biomass Conversion and Biorefinery*, *15*(2), 2673-2684. https://doi.org/10.1007/s13399-023-04827-0

El-Masry, R. M., Talat, D., Hassoubah, S. A., Zabermawi, N. M., Eleiwa, N. Z., Sherif, R. M., Abourehab, M. A. S., Abdel-Sattar, R. M., Gamal, M., Ibrahim, M. S., & Elbestawy, A. (2022). Evaluation of the antimicrobial activity of ZnO nanoparticles against enterotoxigenic *Staphylococcus aureus*. *Life*, *12*(10), Article 1662. https://doi.org/10.3390/life12101662

Emami-Karvani, Z., & Chehrazi, P. (2012). Antibacterial activity of ZnO nanoparticle on Gram-positive and Gram-negative bacteria. *African Journal of Microbiology Research*, *5*(12), 1368-1373. https://doi.org/10.5897/ajmr10.159

Eslami, N., Fasihi, F., Jamalinasab, A., & Ahrari, F. (2021). Biocompatibility of several colloidal solutions containing nanoparticles on human gingival fibroblasts. *Dental Research Journal*, *18*(1), 1-8. https://doi.org/10.4103/1735-3327.310037

Gonçalves, J., Torres, N., Silva, S., Gonçalves, F., Noro, J., Cavaco-Paulo, A., Ribeiro, A., & Silva, C. (2020). Zein impart hydrophobic and antimicrobial properties to cotton textiles. *Reactive and Functional Polymers*, *154*, Article 104664. https://doi.org/10.1016/j.reactfunctpolym.2020.104664

Hamouda, R. A., Alharbi, A. A., Al-Tuwaijri, M. M., & Makharita, R. R. (2023). The antibacterial activities and characterizations of biosynthesized zinc oxide nanoparticles, and their coated with alginate derived from *Fucus vesiculosus*. *Polymers*, *15*(10), Article 2335. https://doi.org/10.3390/polym15102335

Hassanein, T. F., Mohammed, A. S., Mohamed, W. S., Sobh, R. A., & Zahran, M. K. (2021). Optimized synthesis of biopolymer-based zinc oxide nanoparticles and evaluation of their antibacterial activity. *Egyptian Journal of Chemistry*, *64*(7), 3767-3790. https://doi.org/10.21608/ejchem.2021.75677.3709

Indolia, A. P., & Gaur, M. S. (2013). Investigation of structural and thermal characteristics of PVDF/ZnO nanocomposites. *Journal of Thermal Analysis and Calorimetry*, *113*(2), 821-830. https://doi.org/10.1007/s10973-012-2834-0

Jayachandran, A., T.R., A., & Nair, A. S. (2021). Green synthesis and characterization of zinc oxide nanoparticles using *Cayratia pedata* leaf extract. *Biochemistry and Biophysics Reports*, *26*, Article 100995. https://doi.org/10.1016/j.bbrep.2021.100995

Jeong, M., Kwon, S., Hyeon, C., Baek, J., Seong, M., Kim, M., & Lee, D. (2025). Hydrophobic radiative cooling using zein-functionalized polyvinyl alcohol nanofibers with dielectric nanoparticles. *Small*, *21*(45), Article e07295. https://doi.org/10.1002/smll.202507295

Kachoei, M., Divband, B., Tabriz, F. D., Helali, Z. N., & Esmailzadeh, M. (2018). A comparative study of antibacterial effects of mouthwashes containing Ag/ZnO or ZnO nanoparticles with chlorhexidine and investigation of their cytotoxicity. *Nanomedical Journal*, *5*(2), 102-110. https://doi.org/10.22038/nmj.2018.005.007

Kasper, S. H., Hart, R., Bergkvist, M., A. Musah, R., & C. Cady, N. (2016). Zein nanocapsules as a tool for surface passivation, drug delivery and biofilm prevention. *AIMS Microbiology*, *2*(4), 422-433. https://doi.org/10.3934/microbiol.2016.4.422

Khatir, N. M., & Zak, A. K. (2024). Antibacterial activity and structural properties of gelatin-based sol-gel synthesized Cu-doped ZnO nanoparticles; promising material for biomedical applications. *Heliyon*, *10*(17), Article e37022. https://doi.org/10.1016/j.heliyon.2024.e37022

Khier, L., Abdelghani, L., Okba, B., Maouche, D., & Said, L. (2021). X-ray diffraction analysis of kaolin M1 and M2 via the Williamson–Hall and Warren–Averbach methods. *Journal of Chemical Research*, *45*(7-8), 668-673. https://doi.org/10.1177/1747519820984729

Kim, D. H., Kim, J., Lee, C. Y., Hong, M. H., Heo, J. H., & Lee, J. H. (2024). Advancing oral health: the antimicrobial power of inorganic nanoparticles. *Journal of the Korean Ceramic Society*, *61*(2), 201-223. https://doi.org/10.1007/s43207-023-00358-6

Kim, I., Viswanathan, K., Kasi, G., Thanakkasaranee, S., Sadeghi, K., & Seo, J. (2022). ZnO nanostructures in active antibacterial food packaging: Preparation methods, antimicrobial mechanisms, safety issues, future prospects, and challenges. *Food Reviews International*, *38*(4), 537-565. https://doi.org/10.1080/87559129.2020.1737709

Klinbumrung, A., Panya, R., Pung-Ngama, A., Nasomjai, P., Saowalakmeka, J., & Sirirak, R. (2022). Green synthesis of ZnO nanoparticles by pineapple peel extract from various alkali sources. *Journal of Asian Ceramic Societies*, *10*(4), 755-765. https://doi.org/10.1080/21870764.2022.2127504

Küünal, S. (2022). *Plant mediated synthesis of silver-based nanoparticles and their use as antimicrobial agent in environmentally-friendly applications*. [Doctoral Thesis, Tallinn University of Technology]. https://www.rauwel.eu/1/wp-content/uploads/2022-Thesis-Siim-Kuunal.pdf

Ma, J., An, W., Xu, Q., Fan, Q., & Wang, Y. (2019). Antibacterial casein-based ZnO nanocomposite coatings with improved water resistance crafted via double in situ route. *Progress in Organic Coatings*, *134*, 40-47. https://doi.org/10.1016/j.porgcoat.2019.05.007

Macarthur, K. E., Yankovich, A. B., Béché, A., Luysberg, M., Brown, H. G., Findlay, S. D., Heggen, M., & Allen, L. J. (2021). Optimizing experimental conditions for accurate quantitative energy-dispersive X-ray analysis of interfaces at the atomic scale. *Microscopy and Microanalysis*, *27*(3), 528-542. https://doi.org/10.1017/S1431927621000246

Murukesan, S., Varadarajan, S., Jagannathan, R., Rajendran, S., Rajendiran, D., & Balaji, T. M. (2023). Microbial contamination of toothbrush and methods to overcome - A review. *Texila International Journal of Public Health*, *11*(3), Article Art030. https://doi.org/10.21522/TIJPH.2013.11.03.Art030

Naguib, G. H., Al-Hazmi, F. E., Kurakula, M., Al-Dharrab, A. A., Hosny, K. M., Alkhalidi, H. M., Hamed, M. T., Hassan, A. H., Al-Mohammadi, A. M., Alnowaiser, A. M., & Pashley, D. H. (2018). Zein coated zinc oxide nanoparticles: Fabrication and antimicrobial evaluation as dental aid. *International Journal of Pharmacology*, *14*(8), 1051-1059. https://doi.org/10.3923/ijp.2018.1051.1059

Naguib, G. H., El-Aziz, G. S. A., Mously, H. A., Alhazmi, W. A., Alnowaiser, A. M., Hassan, A. H., & Hamed, M. T. (2021). In vitro investigation of the antimicrobial activity of mouth washes incorporating zein-coated magnesium oxide nanoparticles. *Clinical, Cosmetic and Investigational Dentistry*, *13*, 395-403. https://doi.org/10.2147/CCIDE.S327912

Naqvi, Q. ul A., Kanwal, A., Qaseem, S., Naeem, M., Ali, S. R., Shaffique, M., & Maqbool, M. (2019). Size-dependent inhibition of bacterial growth by chemically engineered spherical ZnO nanoparticles. *Journal of Biological Physics*, *45*(2), 147-159. https://doi.org/10.1007/s10867-019-9520-4

Oktavia, A. D., & Rohmawati, L. (2022). Fabrication of Fe_3O_4/ZnO nanocomposite by ultrasonication wave method and its application for antibacterial. *Indonesian Physical Review*, *5*(3), 177-187. https://doi.org/10.29303/ipr.v5i3.175

Osorio, R., Yamauti, M., Osorio, E., Ruiz-Requena, M. E., Pashley, D. H., Tay, F. R., & Toledano, M. (2011). Zinc reduces collagen degradation in demineralized human dentin explants. *Journal of Dentistry*, *39*(2), 148-153. https://doi.org/10.1016/j.jdent.2010.11.005

Pascoli, M., de Lima, R., & Fraceto, L. F. (2018). Zein nanoparticles and strategies to improve colloidal stability: A mini-review. *Frontiers in Chemistry*, *6*, Article 6. https://doi.org/10.3389/fchem.2018.00006

Pillai, S. G., Johnson, L., & Bagde, H. (2023). Chlorhexidine mouthwash in dentistry. *Journal of Nursing Research, Patient Safety and Practise*, *3*(3), 24-29. https://doi.org/10.55529/jnrpsp.33.24.29

Puspasari, V., Ridhova, A., Hermawan, A., Amal, M. I., & Khan, M. M. (2022). ZnO-based antimicrobial coatings for biomedical applications. *Bioprocess and Biosystems Engineering*, *45*(9), 1421-1445. https://doi.org/10.1007/s00449-022-02733-9

Ranimol, G., Paul, C., & Sunkar, S. (2021). Optimization and efficacy studies of Laccase immobilized on Zein-Polyvinyl pyrrolidone nano fibrous membrane in decolorization of acid red 1. *Water Science and Technology*, *84*(10-11), 2703-2717. https://doi.org/10.2166/wst.2021.200

Rao, L. S., Rao, T. V., Naheed, S., & Rao, P. V. (2018). Structural and optical properties of zinc magnesium oxide nanoparticles synthesized by chemical co-precipitation. *Materials Chemistry and Physics*, *203*, 133-140. https://doi.org/10.1016/j.matchemphys.2017.09.048

Rini, A. S., Dewi, R., Yanuar, H., Rati, Y., & Soerbakti, Y. (2025). Controllable zinc oxide micro-flowers utilizing pineapple peel extract. *Letters in Applied NanoBioScience*, *14*(4), 1-8.

Rohmawati, L., Ferdianto, S. P., Ma'arif, M. S., Ardiansyah, F. F., Muadhif, F. I., Setyarsih, W., Supardi, Z. A. I., & Darminto, D. (2025). Enhanced efficiency of dye-sensitized solar cells using ZnO nanoparticle doping Cu from pineapple peel extract with modified natural dye solution. *Eurasian Physical Technical Journal*, *22*(2–52), 42-53. https://doi.org/10.31489/2025N2/42-53

Rohmawati, L., Lailia, L. R., Putri, N. P., Nasir, M., & Darminto, D. (2024a). Characterization of ZnO nanoparticles pineapple skin extract (*Ananas comosus* L.) as photocatalytic activity. *Journal of Water and Environmental Nanotechnology*, *9*(1), 112-123. https://doi.org/10.22090/jwent.2024.01.08

Rohmawati, L., Muadhif, F. I., Putri, N. P., Kusumawati, D. H., Munasir, & Darminto. (2024b). The synthesis of MgO/Zein nanocomposites to improve anti-bacteria characteristics of mouthwash. *EUREKA, Physics and Engineering*, *2024*(2), 178-189. https://doi.org/10.21303/2461-4262.2024.003055

Salamaga, B., Kong, L., Pasquina-Lemonche, L., Lafage, L., von und Zur Muhlen, M., Gibson, J. F., Grybchuk, D., Tooke, A. K., Panchal, V., Culp, E. J., Tatham, E., O'kane, M. E., Catley, T. E., Renshaw, S. A., Wright, G. D., Plevka, P., Bullough, P. A., Han, A., Hobbs, J. K., & Foster, S. J. (2021). Demonstration of the role of cell wall homeostasis in *Staphylococcus aureus* growth and the action of bactericidal antibiotics. *Proceedings of the National Academy of Sciences of the United States of America*, *118*(44), Article e2106022118. https://doi.org/10.1073/pnas.2106022118

Schmitz, F., de Albuquerque, M. B. S., Alberton, M. D., Riegel-Vidotti, I. C., & Zimmermann, L. M. (2020). Zein films with ZnO and ZnO:Mg quantum dots as functional nanofillers: New nanocomposites for food package with UV-blocker and antimicrobial properties. *Polymer Testing*, *91*, Article 106709. https://doi.org/10.1016/j.polymertesting.2020.106709

Setyarsih, W., Rohmawati, L., Ardiansyah, F. F., Maarif, M. S., & Darminto, D. (2025). Photocatalytic activity of ZnO nanoparticles from pineapple skin for degradation of congo red dye. *Trends in Sciences*, *22*(2), Article 9042. https://doi.org/10.48048/tis.2025.9042

Sidhu, A. K., Verma, N., & Kaushal, P. (2022). Role of biogenic capping agents in the synthesis of metallic nanoparticles and evaluation of their therapeutic potential. *Frontiers in Nanotechnology*, *3*, Article 801620. https://doi.org/10.3389/fnano.2021.801620

Sirelkhatim, A., Mahmud, S., Seeni, A., Kaus, N. H. M., Ann, L. C., Bakhori, S. K. M., Hasan, H., & Mohamad, D. (2015). Review on zinc oxide nanoparticles: Antibacterial activity and toxicity mechanism. *Nano-Micro Letters*, *7*(3), 219-242. https://doi.org/10.1007/s40820-015-0040-x

Tiwari, V., Mishra, N., Gadani, K., Solanki, P. S., Shah, N. A., & Tiwari, M. (2018). Mechanism of anti-bacterial activity of zinc oxide nanoparticle against carbapenem-resistant *Acinetobacter baumannii*. *Frontiers in Microbiology*, *9*, Article 1218. https://doi.org/10.3389/fmicb.2018.01218

Wang, M., Buist, G., & van Dijl, J. M. (2022). Staphylococcus aureus cell wall maintenance – the multifaceted roles of peptidoglycan hydrolases in bacterial growth, fitness, and virulence. *FEMS Microbiology Reviews*, *46*(5), Article fuac025. https://doi.org/10.1093/femsre/fuac025

Zare, M., Namratha, K., Ilyas, S., Sultana, A., Hezam, A., L, S., Surmeneva, M. A., Surmenev, R. A., Nayan, M. B., Ramakrishna, S., Mathur, S., & Byrappa, K. (2022). Emerging trends for ZnO nanoparticles and their applications in food packaging. *ACS Food Science and Technology*, *2*(5), 763-781. https://doi.org/10.1021/acsfoodscitech.2c00043